УДК 621.314.572 DOI: https://doi.org/10.15407/techned2023.05.014

EVOLUTION AND DISSEMINATION OF SPECIALIZED STRATEGIES, METHODS, AND TECHNIQUES OF SYNCHRONOUS PULSEWUDTH MODULATION FOR CONTROL OF VOLTAGE SOURCE INVERTERS AND INVERTER-BASED SYSTEMS

V. Oleschuk
Institute of Power Engineering of Technical University of Moldova,
Academy Str., 5, Kishinau, MD-2028, Moldova.
E-mail: oleschukv@hotmail.com

This publication provides a brief historical overview of the development of methods and techniques of pulsewidth modulation (PWM) for voltage source inverters, published mainly in Ukrainian publishing houses and in Ukrainian periodicals. Accent has been done to review of results of investigation of alternative methods and techniques of synchronous space-vector-based multi-zone PWM for inverters with low switching frequency. In particular, in the mentioned publications, the basic strategies, schemes, and algorithms of synchronous multi-zone modulation have been further developed, modernized, modified, and disseminated in relation to new promising topologies of power conversion systems, including: two-inverter-based electric drives with open-end winding of electrical motor; dual three-phase electric drives of symmetrical and asymmetric types; powerful six-phase systems based on four inverters, and two-inverter-based and three-inverter-based photovoltaic installations with multi-winding transformer. It is shown that the developed schemes and algorithms of synchronous space-vector PWM, applied for control of inverter-based systems, provide continuous synchronization and symmetry of basic voltage waveforms of systems during the whole control range including zone of overmodulation of inverters. It provides minimization of even harmonics and undesirable subharmonics (of the fundamental frequency) in spectra of the basic voltages of systems, leading to reducing of losses in systems and to increasing of its efficiency. Based on a comparative analysis of the integral spectral characteristics of the phase and line voltages of systems, recommendations are formulated for the rational choice of schemes and algorithms of synchronous modulation for the relevant installations, depending on the modes of their operation. References 30, tables 2, figures 25.

Keywords: voltage source inverter, modulation strategy, adjustable speed ac drive, photovoltaic installation, six-phase system, voltage synchronization, voltage spectra.

Introduction. Power electronic converters are currently one of the most common electric power installations, providing energy savings and improving the quality of technological processes in various fields of industry, utilities, electric transport, renewable energy systems, etc. [1, 2].

The structure of the power circuits of power converters includes powerful semiconductor switches (transistors and thyristors) operating in a pulsed mode. So, characteristics of these systems depend on the used methods of pulsewidth modulation (PWM) of the control signals of converters [3 – 5].

Development of theory and practice of pulsewidth modulation for power converters began at the 60s years of the last century. In accordance with this fact, it is necessary to mention, that from the beginning of the 70s Institute of Electrodynamics of the Academy of Sciences of Ukraine was put in charge on research on power conversion systems, in the range of the former USSR, including investigation of methods and techniques of pulsewidth modulation for power converters. So, it has been marked by remarkable contribution in the development of novel strategies, methods, and techniques of PWM by Ukrainian researchers and engineers [6 – 16].

In particular, in the last quarter of the 20th century activity of researchers has been concentrated on investigation of both pulse-width modulation and pulse-amplitude modulation [6 – 11], and it is necessary to mentioned specially about study of methods and techniques of space-vector-based modulation for voltage source inverters for drive applications ([9], and this publication is one of the first publications in the world on this topic).

* ORCID ID: https://orcid.org/0000-0002-7413-4867

Latter, at the beginning of the 21st century, methods, schemes, and techniques of space-vector-based PWM has been further developed and analyzed [12 – 16]. Rational techniques of determination of stationary states of power switches of inverters have been investigated, with definition of the order of their alternation and relative durations on the cycle of modulation for the formation of undistorted output voltage of inverters with the maximum modulation index. Comparison of vector and scalar approaches to different methods of PWM has been carried out. Detailed investigation of operation of inverters in the zone of overmodulation has been done.

At the same time, some specialized methods and techniques of pulsewidth modulation have been elaborated and studied at the beginning of the 21st century. In particular, in order to provide continuous synchronization and symmetry of the output voltage and current of voltage source inverters with low switching frequency, alternative method of synchronous multi-zone modulation for three-phase inverters, based on space-vector approach, has been elaborated, investigated, and disseminated to different perspective topologies of systems and installations [17 – 22].

So, this publication presents a brief overview of the results of research in the field of development and dissemination of the method of synchronous multi-zone PWM of inverters with application to different topologies of inverter-based ac drives and photovoltaic installations, published mainly in the journal "Technical Electrodynamics" during 2002-2022.

Method, schemes, and techniques of synchronous multi-zone space-vector modulation for three-phase inverters. In order to provide continuous synchronization of voltage waveforms of inverters with space-vector-based PWM, novel approach has been proposed for synthesis of the output voltage of three-phase voltage source inverters [17]. The PWM process is characterized here by smooth pulses-ratio changing and by quarter-wave symmetry of the voltage waveforms during the whole control range including the zone of overmodulation. Generalized properties of both conventional asynchronous and proposed synchronous methods of feedforward space-vector PWM are presented in Table 1 [17]. In comparison with conventional space-vector scheme of PWM the proposed method is based on representation of pulse-widths of the signals of the inverter as a function of the fundamental frequency and switching frequency of inverters. There can be used either accurate trigonometric or simplified algebraic control functions for generation of the pulse patterns. The equations presented in Table I correspond to scalar control mode of operation of adjustable speed drives.

Table 1 [17].

Control (modulation) parameter	**Conventional asynchronous PWM**	**Proposed method of synchronous modulation**	
Current and max parameter	Current & max voltage V and V_m	Current & maximum fundamental frequency F and F_m	
Modulation index m	V / V_m	F / F_m	
Duration of sub-cycles	T	τ	
Centre of the k-signal	α_k (angles/degr.)	$\tau(k-1)$ (sec)	
Switch-on durations	$T_{ak} = mT[\sin(60^0 - -\alpha_k) + \sin\alpha_k]$ $t_{ak} = mT\sin\alpha_k$ $t_{bk} = mT\sin(60^0 - \alpha_k)$	Algebraic PWM $\beta_k = 1.1m\tau[1 - A(k-1)\tau F]$ $\gamma_k = \beta_{i-k+1}[0.5 - 6(i-k)\tau F]$ $\beta_k - \gamma_k$	Trigonometric PWM $\beta_k = 1.1m\tau \times \cos[(k-1)\tau]$ $\gamma_k = \beta_{i-k+1}[0.5 - 0.9\tan(i-k)\tau]$ $\beta_k - \gamma_k$
Switch-off states (zero voltage)	$t_{0k} = T - t_{ak} - t_{bk}$	$\lambda_k = \tau - \beta_k$	
Special parameters providing synchronization of the process of PWM		λ' (clock-point notches) β'' (signals, the next to λ') F_i (boundary frequencies, where $\lambda' \Rightarrow 0$ and $\beta'' \Rightarrow 0$)	

The process of calculation the parameters of control pulse signals for three-phase drive inverters with synchronous multi-zone PWM is based on the continuous determination of the values of

$F_i = [6(2i-1)\tau]^{-1}$ and $F_{i-1} = [6(2i-3)\tau]^{-1}$ of intermediate frequencies between the control sub-zones of system (as a function of the duration of the clock sub-interval τ), and in calculation of special coefficient $K_S = [1-(F-F_i)/(F_{i-1}-F_i)]$, which is correcting coefficient for continuous determination of the λ' and β'' control signals.

Fig. 1 shows switching state sequence (with the corresponding control signals) of three-phase inverter with continuous scheme of synchronous PWM (upper curve, the corresponding control signals are presented here), and also the corresponding parts of the phase voltages and of line voltage for a quarter-period of the output voltage of inverter [17]. In Fig. 1, the conventional designation for state sequences for the switches of the phases ***abc*** of the inverter is used: **1** – 100; **2** –110; **3** –010; **4** –011; **5** –001; **6** –101; **7**–111; **0** –000 (‘1’ -switch-on state, ‘0’ –switch-off state) [17].

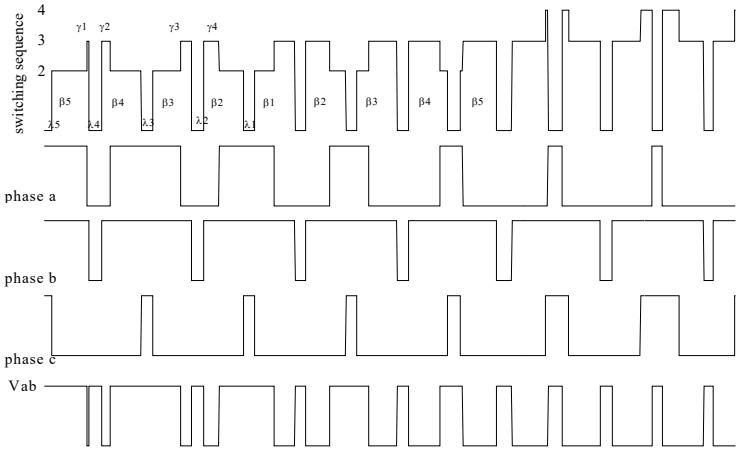

Fig. 1 [17]

Fig. 2 shows, as an example, two half-waves of the line-to-line output voltage of inverter with synchronous PWM, and presents also the corresponding spectra of its line voltages (*N* – number of pulses in a half-wave of the line voltage) [17]. The presented voltage spectra include only odd (non-triplen) voltage harmonics, and even harmonics and subharmonics are illuminated from the spectrum during the whole control range due to the proposed method of voltage synchronization [17].

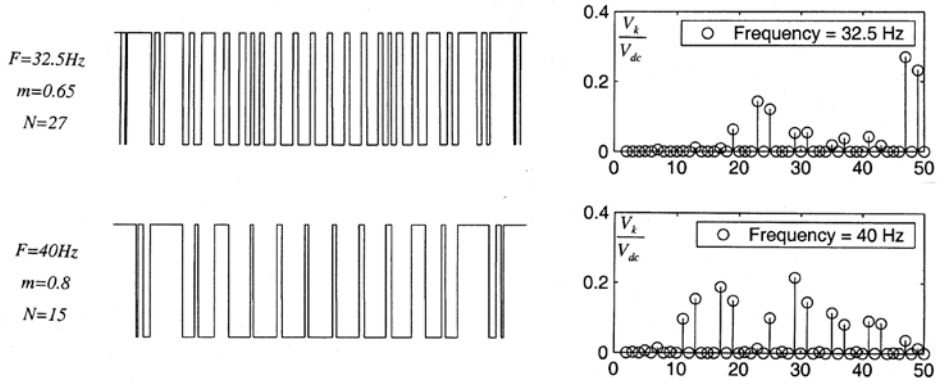

Fig. 2 [17]

Open-end winding drive systems with two inverters with synchronous space-vector PWM. One of the interesting and perspective topologies of power converters are cascaded (dual) two-level converters which utilize two standard three-phase voltage source inverters [18, 23]. The structure of adjustable speed drive based on cascaded inverters is constructed by splitting the neutral connection of the induction motor and connecting both ends of each phase coil to a two-level inverter. In this case cascaded converters are capable of producing voltages which are identical to those of three-level and four-level converters [18].

Fig. 3 presents the basic structure of a dual inverter-fed open-end winding induction motor drive, where INV1 and INV2 are standard three-phase voltage source inverters [18, 23]. The single power supply is used for both inverters in this case, because elimination of the common-mode voltages is provided by the specialized

scheme of modulation. Fig. 4 shows the switching state vectors of two inverters, which provide elimination of the zero sequence currents in drive system [18]. All control and output signals of the inverters INV1 and INV2 have mutual phase shift in 120^0 in accordance with the presented scheme of space-vector modulation. Each inverter generates in this case alternating common-mode voltage, but these common-mode voltages do not cause the zero sequence currents in the machine phase winding, because these voltages compensate each other [18].

Fig. 5 presents the corresponding voltage waveforms of the drive system with continuous synchronous PWM (Fig. 5, *a*, fundamental frequency $F = 40$ *Hz*, modulation index $m = 0.8$ in this case) and shows also spectrum of the phase voltage (Fig. 5, *b*) [18]. Average switching frequency of inverters $F_s = 1$ *kHz*. Fig. 6 illustrates corresponding voltage waveforms and spectrum of the phase voltage for dual-inverter system controlled by algorithms of discontinuous synchronous PWM with the 30-degrees non-switching intervals [18]. The spectra of the phase voltage of the system, presented in Fig. 5, *b* and Fig. 6, *b*, contain only odd harmonics without the triplen components.

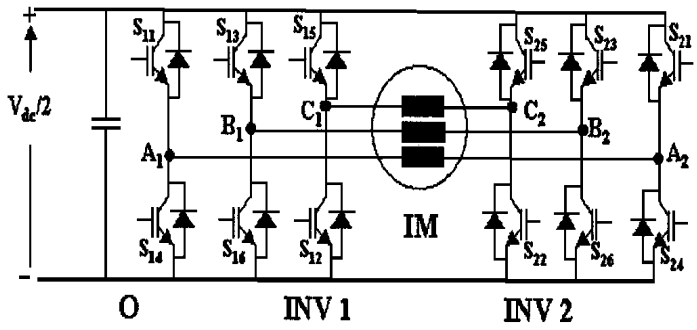

Fig. 3 [18]

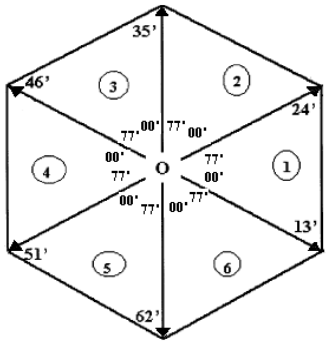

Fig. 4 [18]

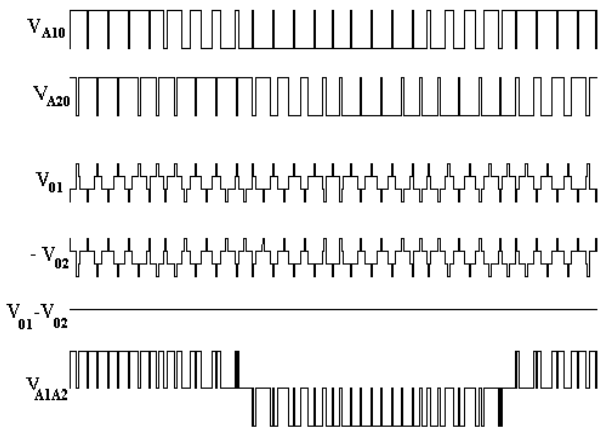

a

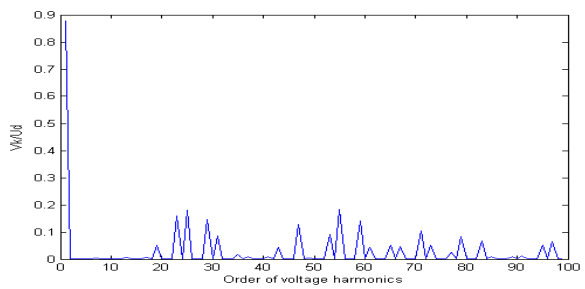

b

Fig. 5 [18]

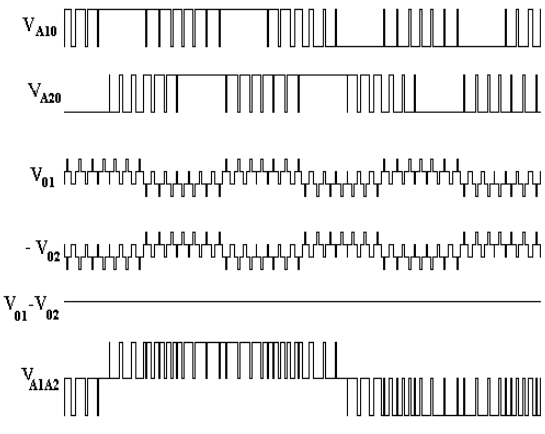

a

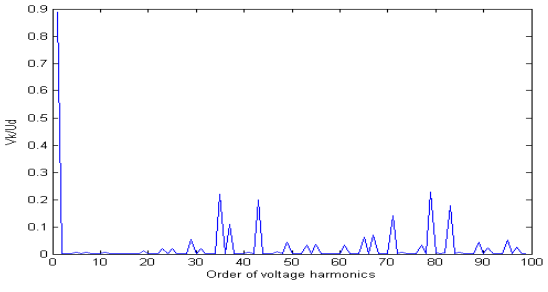

b

Fig. 6 [18]

Fig. 7 presents results of calculation of Weighted Total Harmonic Distortion factor ($WTHD = (1/V_1)\sqrt{\sum_{i=2}^{1000}(V_i/i)^2}$) for dual-inverter system with continuous (CPWM) and discontinuous (DPWM) versions of synchronous modulation. Average switching frequency for each presented version of pulsewidth modulation is equal to *1 kHz*, control mode corresponds here to standard *V/F* control [18]. Presented in Fig. 7 spectral characteristics show some advantage regarding spectra of the phase voltage in the systems with continuous PWM at low modulation indexes, and advantage of discontinuous scheme of synchronous PWM at higher values of modulation index.

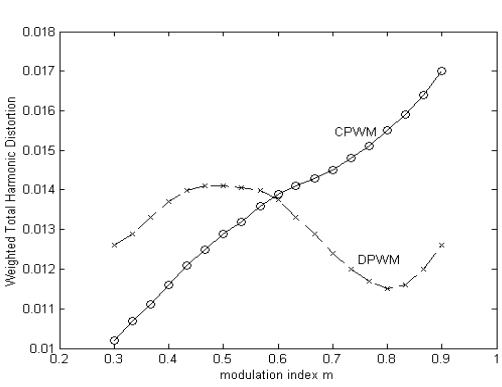

Fig. 7 [18]

Dual three-phase inverted systems controlled by algorithms of synchronous PWM. Application of dual three-phase inverter-based drives can be perspective for the systems with an increased power rating [19], [24] – [25]. As an example of asymmetrical dual three-phase traction drive system with two dc voltage sources, Fig. 8, *a* shows structure of the electrical vehicle system on the base of the dual three-phase induction motor supplied by two inverters with two different dc links: 1) Battery dc link with the V_{dc1} voltage, and 2) Fuel Cell dc link with the V_{dc2} voltage [19], [24]. The induction machine has in this case two sets of winding spatially shifted by 30 electrical degrees with isolated neutral points (Fig. 8, *b*) [19], [24].

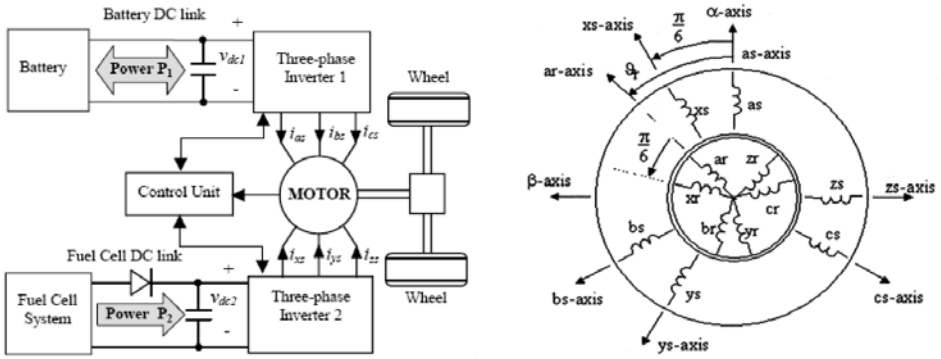

a ***b***

Fig. 8 [19, 24]

Two neutral-point-clamped (NPC) inverters can be used in dual three-phase systems with an increased power level. Fig. 9, *a* presents basic topology of NPC inverter (of the first inverter in Fig. 8, *a* with the phases ***a, b, c***). Fig. 9, *b* shows switching state vectors of the inverter. In accordance with the diagram presented in Fig. 9, *b*, specialized control scheme has been applied for adjustment of NPC inverters of dual three-phase system, which is based on the using of only seven voltage vectors, marked by the big arrows in Fig. 9, *b*. It allows providing elimination of undesirable common-mode voltage in a three-phase load [19].

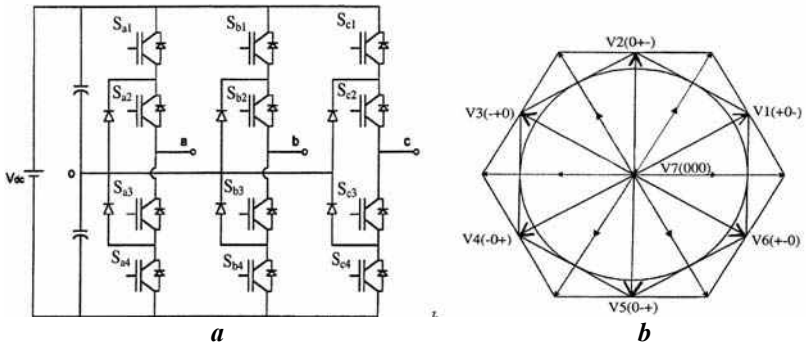

a ***b***

Fig. 9 [19]

Control of asymmetrical dual three-phase drives is based on the 30^0-phase-shift of the signals of two inverters with the phases ***a, b, c***, and ***x, y, z*** [19], [24]. Fig. 10 – Fig. 11 present basic voltage waveforms (phase voltages V_{as} and V_{xs} and its useful components V_{sa} and V_{sb}, common-mode and line voltages V_0 and V_{ab}, and spectrum of the V_{as} voltage) of dual three-phase system with two dc sources with equal voltages ($V_{dc1} = V_{dc2}$) under standard scalar *V/F* control mode [19]. In particular, Fig. 10 illustrates behavior of dual three-phase system with NPC inverters controlled by continuous synchronous PWM, and Fig. 11 presents basic voltage waveforms and spectrum of the phase voltage for system with algorithms of "direct-direct" synchronous PWM [19]. The switching and fundamental frequencies of each NPC inverter are equal to $F_s = 900\ Hz$ and $F = 42\ Hz$ ($m_1=m_2=0.84$).

The motor phase and line voltages of dual three-phase system with NPC inverters controlled by algorithms of synchronous PWM have symmetry during the whole control range, and its spectra do not include even harmonics and sub-harmonics. The described strategy of control of dual NPC inverters provides elimination of common-mode voltage both in each inverter and in the load, which is leading to an increase of the reliability and life span of adjustable speed drives with modulated power converters.

Fig. 12 presents calculation results of the Weighted Total Harmonics Distortion factor ($WTHD = (1/V_1)(\sum_{k=2}^{1000}(V_k/k)^2)^{0.5}$) versus modulation index m for the useful component V_{sa} of the motor phase voltage of asymmetrical dual three-phase system with two NPC inverters controlled by algorithms of continuous (CPWM), discontinuous (DPWM) and "direct-direct" (DDPWM) schemes of synchronous multi-zone PWM during scalar *V/F* control ($V_{dc1} = V_{dc2}$, $m_1 = m_2 = m = 0.3–0.9$) [19]. Average switching frequency of each inverter is equal to $F_s = 900\ Hz$ [19].

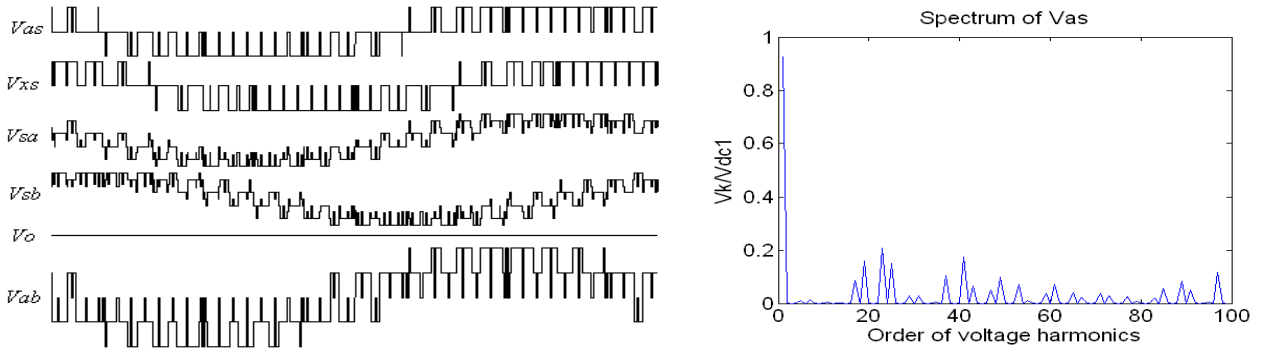

Fig. 10 [19]

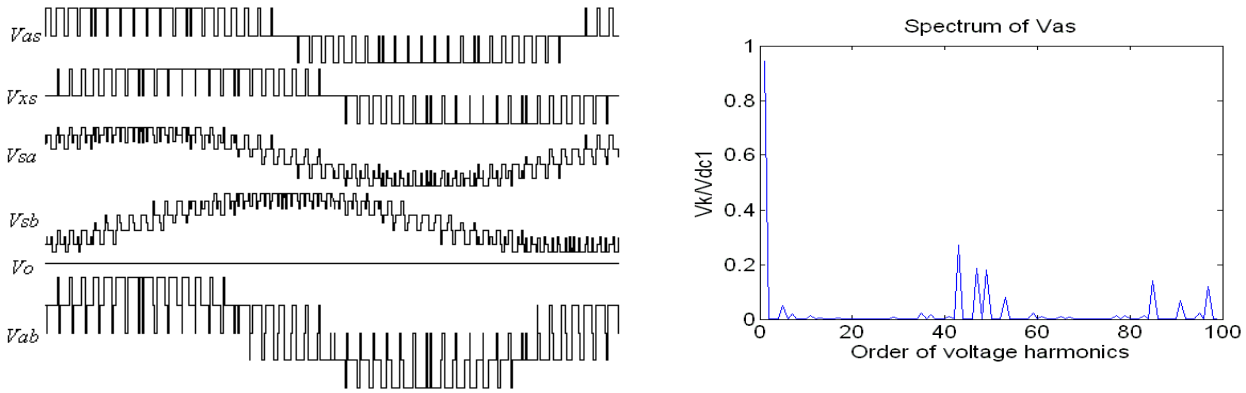

Fig. 11 [19]

Results of analysis of spectral composition of the useful component of motor phase voltage show that at low modulation indices *WTHD* factor is better for systems controlled by continuous and "direct-direct" schemes of synchronous PWM, and at the medium and high modulation indices, discontinuous and "direct-direct" versions of synchronous PWM provide the better *WTHD* factor of the V_{sa} voltage.

Six-phase systems based on four inverters with synchronous multi-zone PWM. Multiphase, and, in particular, six-phase induction motor drives are a subject of increasing interest in the last years due to some advantages compared with conventional three-phase drives [20, 26, 27]. One of the most perspective applications of six-phase systems lies in the field of high power/high current systems), which are characterized by relatively low switching frequency of power switches of inverters.

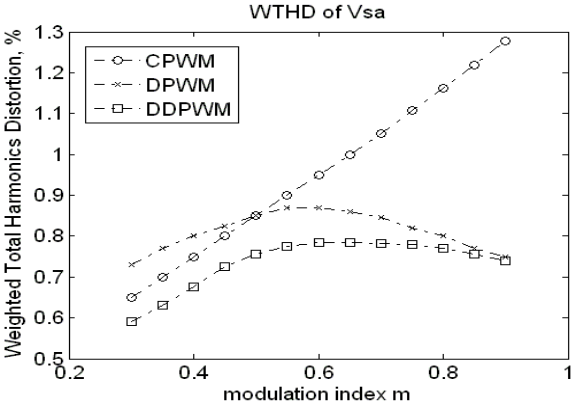

Fig. 12 [19]

Fig. 13 shows one of perspective structure of six-phase four-inverter-based system, consisting of two groups of two inverters (**INV1+INV2** and **INV3+INV4**), supplying the open-end windings of asymmetrical dual three-phase (six-phase) motor. The induction machine has in this case two sets of winding spatially shifted by 30 electrical degrees [20, 26].

Control of four three-phase inverters supplying asymmetrical six-phase induction motor has some specific peculiarities. In particular, all inverters are grouped into two groups with two cascaded inverters in each group, and each inverter group is connected with the corresponding open-end windings of six-phase induction motor. Synchronous symmetrical control of the output voltage of each inverter of each inverter group by algorithms of synchronous multi-zone PWM provides synchronous symmetrical regulation of voltage at the corresponding windings of induction machine. Rational phase shifting between the output voltages of two inverters in each inverter group is equal in this case to one half of the switching interval (sub-cycle) [20].

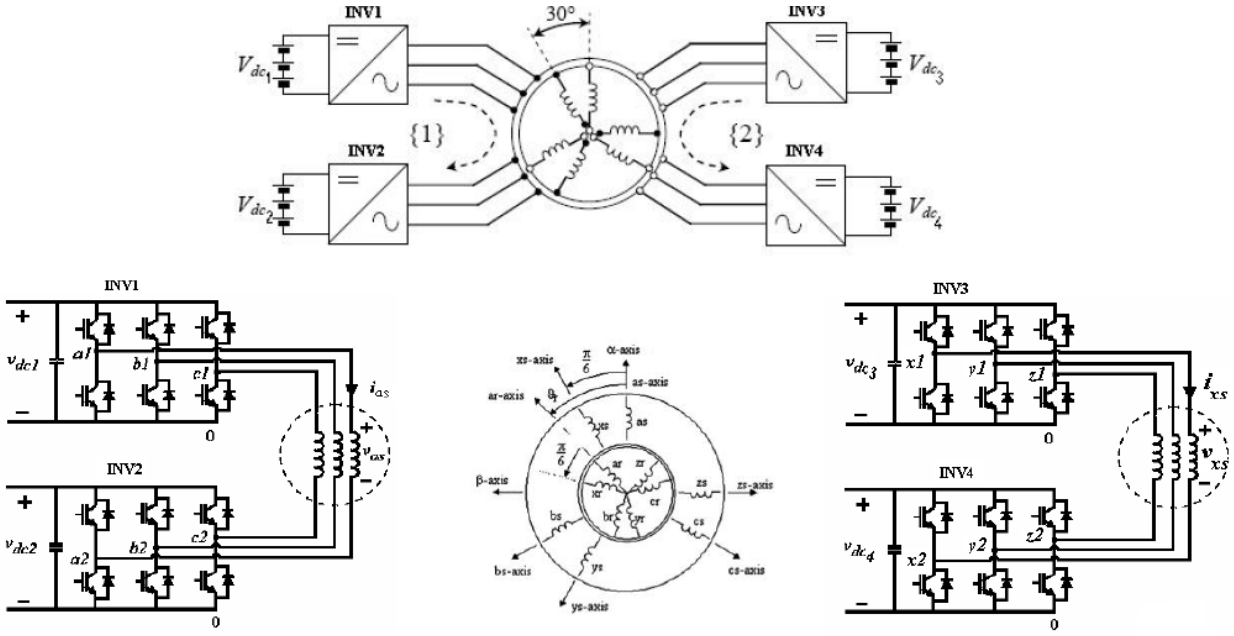

Fig. 13 [20]

As an illustration of operation of six-phase system with four inverters controlled by algorithms of synchronous PWM with equal voltages of the all dc-sources ($V_{dc1} = V_{dc2} = V_{dc3} = V_{dc4}$), Figs. 14 – 15 present basic voltage waveforms (pole voltages V_{a1}, V_{a2}, V_{x1}, V_{x2}, line-to-line voltages V_{a1b1}, V_{x1y1}, and the phase voltages V_{as} and V_{xs} (with the spectrum of the V_{as} voltage)) of two groups of inverters, controlled by algorithms of continuous (Fig.14) and discontinuous with the 30^0-non-switching intervals (Fig. 15) synchronous PWM [20]. The fundamental and switching frequencies of each inverter are equal correspondingly to $F = 35$ *Hz* and $F_s = 1000$ *Hz*, modulation indices of all inverters are equal to $m_1 = m_2 = m_3 = m_4 = 0.7$ in this case. The phase output voltage of the system has nine levels (like output voltage of three-level neutral-point-clamped inverter) in this control mode. In particular, the presented voltage waveforms have symmetry, and its spectra do not contain even harmonics and sub-harmonics.

In order to compare characteristics of asymmetrical six-phase systems on the base of two inverters (standard topology of the system), and on the base of four inverters (topology of six-phase system presented in Fig. 13 [20]), Fig. 16 presents calculation results of Weighted Total Harmonic Distortion factor (*WTHD*) versus modulation index *m* for the motor phase voltage V_{as} ($WTHD = (1/V_{as_1})(\sum_{k=2}^{1000}(V_{as_k}/k)^2)^{0.5}$ for six-phase system controlled by algorithms of continuous (CPWM) and discontinuous (DPWM) schemes of synchronous multi-zone PWM. In particular, DC-voltage magnitudes are equal in this case for all DC-sources, so,

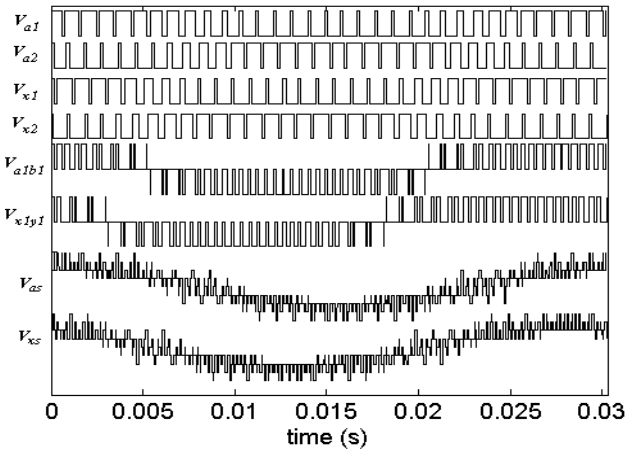

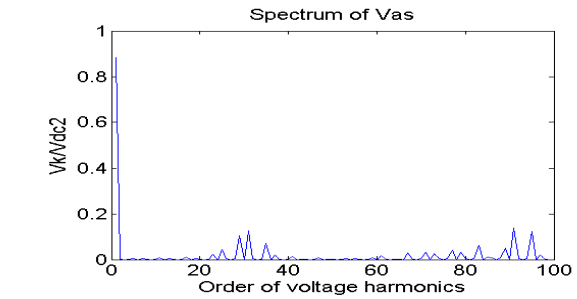

Fig. 14 [20]

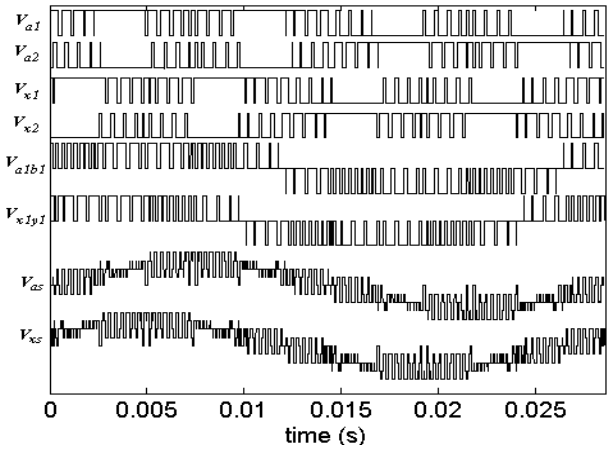

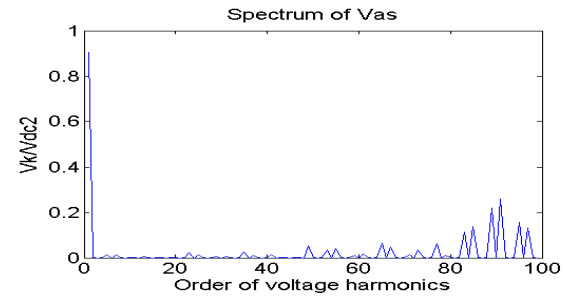

Fig. 15 [20]

modulation indices of all inverters are equal too [20]. Control mode of drive system corresponds here to scalar *V/F* control, and average switching frequency of each inverter is equal to $F_s = 1000\ Hz$. The presented results show, that integral spectral characteristics of the phase voltage of six-phase system on the base of four inverters are much better, than of the system on the base of two inverters.

Fig. 17 presents results of analysis of spectral composition of the phase voltage *Vas* of six-phase system on the base of four inverters with both continuous (CPWM) and discontinuous (DPWM) versions of synchronous PWM for the case of non-equal magnitudes of DC-voltages. In particular, for this case $V_{dc1} \neq V_{dc2}$ and $V_{dc3} \neq V_{dc4}$, but $V_{dc1}=V_{dc3}$ and $V_{dc2}=V_{dc4}$ [20]. Two basic control modes have been analyzed:
1) $V_{dc1} = 0.9\ V_{dc2}$, $V_{dc3} = 0.9\ V_{dc4}$, $K_{dc} = 0.9$; 2) $V_{dc1} = 0.7\ V_{dc2}$, $V_{dc3} = 0.7\ V_{dc4}$, $K_{dc} = 0.7$.

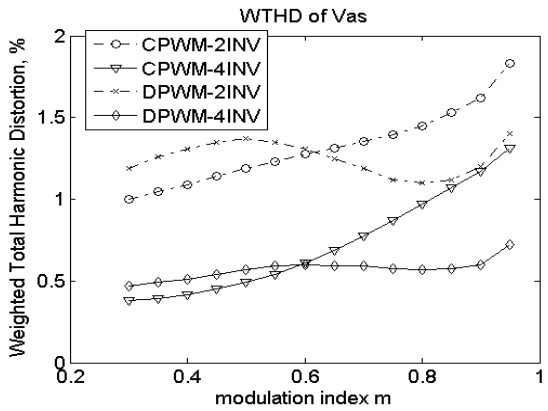

Fig. 16 [20]

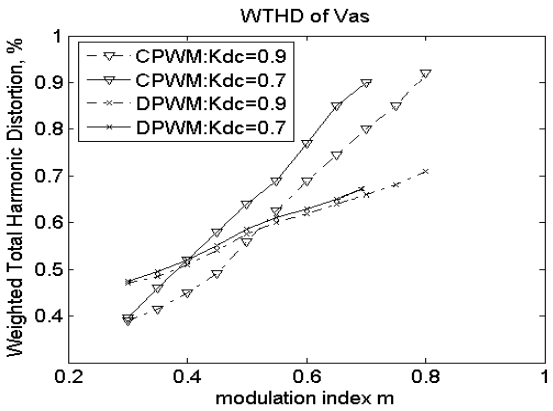

Fig. 17 [20]

The presented results show, that a value of the *WTHD* factor of the phase voltage of six-phase system on the base of four inverters controlled by algorithms of discontinuous synchronized PWM is not strongly sensitive to relative magnitudes of DC-voltages.

Grid-tied photovoltaic system based on two inverters controlled by schemes of synchronous PWM. Besides adjustable speed ac drives, photovoltaic systems are between perspective areas of application of the dual-inverter topology [21, 28, 29]. In particular, Fig. 18 presents dual inverter system supplied by two insulated strings of photovoltaic panels with the resulting dc voltages V_L and V_H [21, 28]. Dual inverters are connected to a grid by a three-phase transformer with the open winding configuration on primary side, and this configuration is one of the most suitable for photovoltaic systems with a higher power range, allowing also galvanic isolation between low-voltage photovoltaic panels and the power grid.

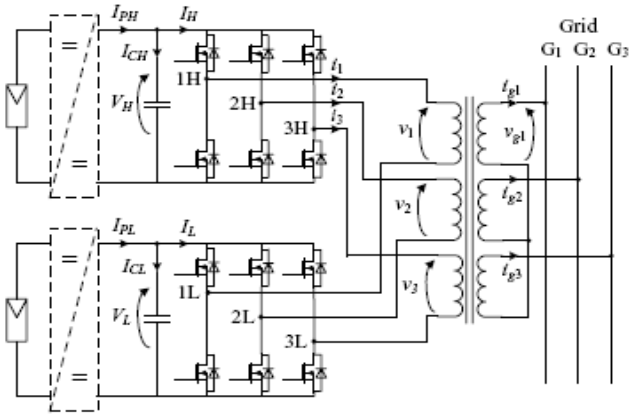

Fig. 18 [21,28]

In order to increase effectiveness of operation of dual three-phase systems on the base of two inverters supplied by isolated DC-sources (with equal or different voltages), it is rational to adjust continuously switching frequency of each modulated inverter in function of voltage magnitude of DC-sources (under condition of similar switching losses of two inverters) [21].

Synchronous control of the output voltage of each inverter of dual-inverter-based system in accordance with algorithms of synchronous PWM provides synchronous symmetrical regulation of the phase voltages V_1, V_2 and V_3 of the system. Rational phase shift between output voltage waveforms of the two inverters in the case of equal dc-links voltages (V_H=V_L) is equal to one half of the switching interval (sub-cycle) [21], and in the case of different dc voltages (and different switching frequencies of two inverters) this shift should be equal to average value of the halves of the corresponding switching intervals.

To illustrate processes in photovoltaic system on the base of cascaded inverters with controlled switching frequencies, supplied by two isolated DC-sources with equal voltages (V_L =V_H,), Fig. 19 – Fig. 20 present results of simulation of PV system with both continuous (Fig. 19) and discontinuous (Fig. 20) versions of synchronous PWM [21].

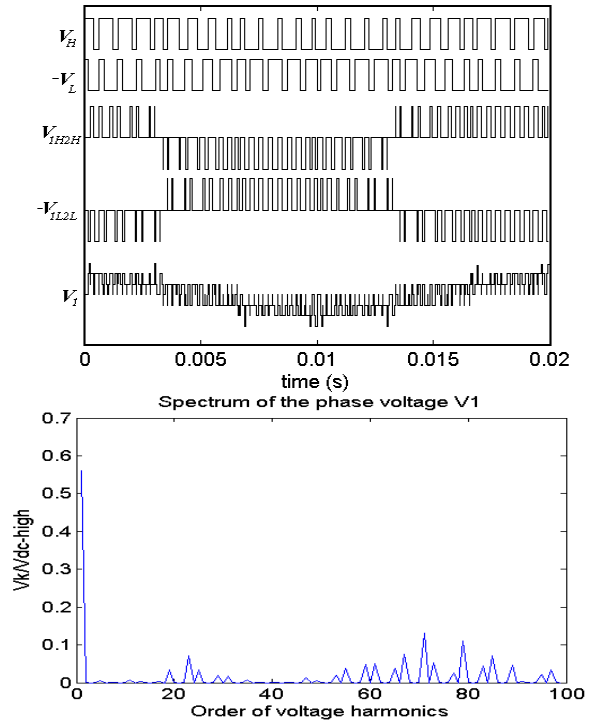

Fig. 19 [21]

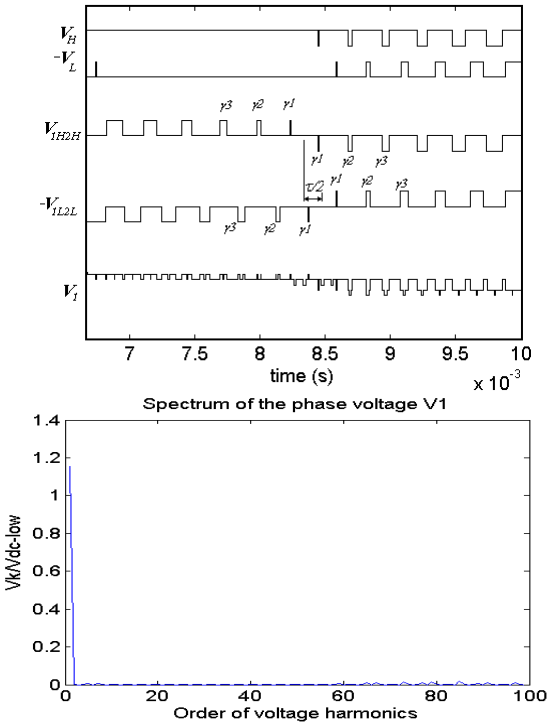

Fig. 20 [21]

Fig. 19 shows basic voltage waveforms of the system with continuous synchronous PWM with high DC-link voltage (V_L=V_H=*Vdc-high*) during period of the fundamental frequency F =50 Hz (switching frequency F_s = 1.2 kHz and modulation index m = 0.45 are relatively low here). It presents also spectrum of the phase voltage V_1 for this control mode [21].

Fig. 20 presents detailed (inside the 60^0-interval) basic voltage waveforms of the system, and spectrum of the phase voltage V_1 for system with discontinuous synchronous PWM, operating under low dc voltage (V_L=V_H=*Vdc-low* (*Vdc-low=0.5Vdc-high*), in particular, it can corresponds to low level of solar irradiance). And this control regime is characterized by relatively high values of switching frequency F_s = 2.4 kHz and modulation index m=0.9. So, waveforms of the phase voltage of the system are characterized in this case much better spectral composition than for the systems with relatively high dc-voltages and lower switching frequencies of inverters [21].

Fig. 21 presents the calculation results of Total Harmonic Distortion factor (*THD*) for the phase voltage V_1 in function of modulation index $m = m_1 = m_2$, of the dual-inverter system on the base of two inverters with equal DC voltages ($V_H = V_L$), controlled by algorithms of continuous (CPWM) and discontinuous (DPWM) schemes of synchronous modulation. *THD* factor ($THD = (1/V_{1_1})\sqrt{\sum_{k=2}^{40} V_{1_k}^2}$) has been calculated until the 40-th low-order (k-th) voltage harmonic. The fundamental frequency of the system is F = 50 Hz, and *THD* factor has been calculated for two values of the average switching frequency of each modulated inverter: F_s = 1.2 kHz and F_s = 2.4 kHz [21].

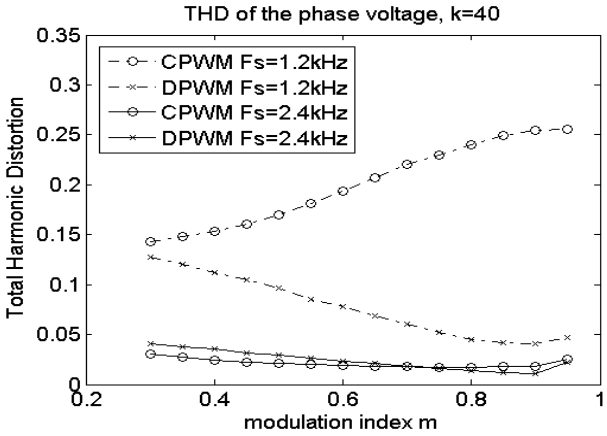

Fig. 21 [21]

The presented in Fig. 21 calculation results show big dependence of *THD* factor on switching frequency of inverters. So, the analyzed scheme of flexible control of switching frequency of dual inverters in function of dc voltages (voltages of two strings of photovoltaic panels) during fluctuation of solar irradiance can improve strongly effectiveness of processes of photovoltaic generation in these systems.

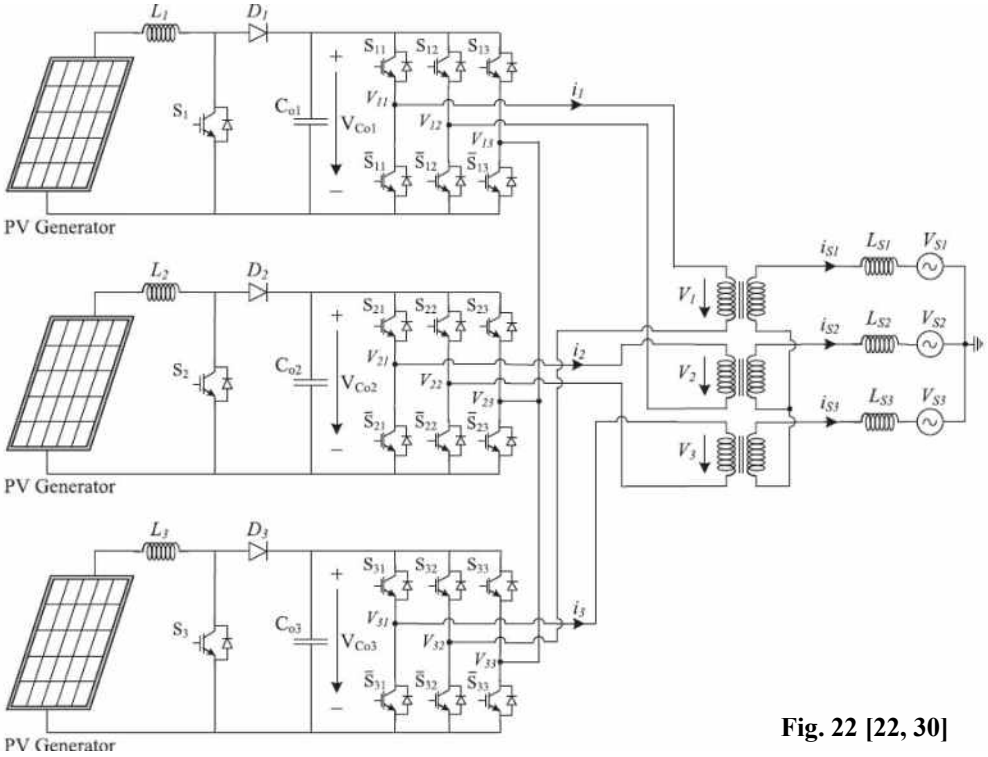

Fig. 22 [22, 30]

Transformer-based photovoltaic system with three inverters with synchronous PWM. Solar-energy-based photovoltaic (PV) renewable energy systems are ones of the most rapidly growing directions of research, implementation, and application between renewable sources of electrical energy [1, 22]. Fig. 22 presents one of perspective configuration of transformer-based grid-connected PV system consisting from three three-phase inverters, outputs of which are specifically connected to the corresponding inverter-side windings of the power transformer [22, 30].

Based on the development of the methodology of synchronous space-vector modulation, and properties of three-inverter-based PV system ([22, 30]), Table 2 presents set of modified control dependences for the presented PV installation allowing synchronous and symmetrical regulation of winding voltages during adjustment of the system, including control modes in the case of fluctuation of frequency of electrical grid [22]. In this Table F is fundamental frequency of electric grid (usually F = 50Hz with some small fluctuations), m is coefficient of modulation of inverters, V_{11} - V_{33} are pole voltages of three inverters.

In accordance with the used control and modulation strategy, control signals of three two-level inverters are shifted by 120^0, and additional mutual phase shift between control pulse signals of three inverters is equal to 1/3 of the width of switching sub-cycle [22].

Fig. 23 – Fig. 24 present results of simulation of PV installation controlled by algorithms of synchronous space-vector PWM, and show, in the relative scale, pole voltages V_{11}, V_{12} and V_{13} of the first inverter, line voltages of the first and the second inverters ($V_{12} - V_{13}$) and ($V_{21} - V_{23}$), and winding voltage V_2 of multi-winding power transformer. It presents also spectral composition of the line ($V_{21} - V_{23}$) voltage, and of the winding voltage V_2 [22]. The fundamental frequency of the output voltage of inverters is equal to F=50 Hz, and the averaged switching frequency of inverters is equal to F_s = 1120 Hz in these cases.

Table 2 [22]

Switching frequency F_s Switching sub-cycle τ	Parameters of control signals and of the output voltage of inverters	Instantaneous values of winding voltages V_1, V_2, and V_3 of system
$F_{s(CPWM)} = F(6n-3)$ $\tau_{CPWM} = 1/2F_s = 1/[6F(2n-1)]$ $F_{s(DPWM)} = F(8n-5)$ $\tau_{DPWM} = 1/[6F(2n-1.5)]$ where n=2,3,4….	$\beta_1 = 1.1m\tau$ $\beta_j = \beta_1 \cos[(j-1)\tau]$ $\gamma_j = \beta_{n-j+1}\{0.8 - 0.5\tan[(n-j)\tau]\}$ $\lambda_j = \tau - (\beta_j + \beta_{j+1})/2$	$V_1 = V_{11} - V_{13} - V_{32} + V_{33}$ $V_2 = V_{21} - V_{23} - V_{12} + V_{13}$ $V_3 = V_{31} - V_{33} - V_{22} + V_{23}$

Fig. 23 shows basic voltage waveforms and spectra of the winding voltage of PV system with inverters controlled by the scheme of continuous synchronous PWM (CPWM), coefficient of modulation of inverters is equal to m = 0.6. Fig. 24 presents the corresponding diagrams for PV system with inverters controlled by algorithms of discontinuous modulation with the 30-degrees non-switching intervals (DPWM30) [22].

Simulation results, presented in Figs. 23 – 24, show, that for the analyzed control modes both line voltages and winding voltages have quarter-wave symmetry and are characterized by the absence in its spectra of even harmonics and sub-harmonics (of the fundamental frequency) [22].

Total Harmonic Distortion (*THD*) factor of the winding voltage V_2 of the analyzed PV system (with average switching frequency of inverters equal to 1120 Hz), has been determined and presented in Fig. 25, *a, b* for the cases for two values of the maximum number of calculated low-order harmonics (k-th harmonics) – k=40 (Fig. 25, *a*), and k=100 (Fig. 25*, b*) [22]:

$$THD = (1/V_{2_1})\sqrt{\sum_{k=2}^{40} V_{2_k}^2} \quad \text{(Fig. 25, } a\text{)}; \qquad THD = (1/V_{2_1})\sqrt{\sum_{k=2}^{100} V_{2_k}^2} \quad \text{(Fig. 25, } b\text{)}.$$

The presented diagrams show a big dependence of the value of *THD* factor on number of voltage harmonics, taking into account during determining *THD*. But for the both cases of determining of *THD* factor, presented in Fig. 25, *a* (k=40) and in Fig. 25, *b* (k=100), better values of *THD* factor can be provided by the using of algorithms of discontinuous PWM (DPWM30 and DPWM60) for control of triple inverters of PV installation. In any case, the use of algorithms of synchronous space-vector PWM insure improved harmonic composition of winding voltage, providing the corresponding reduction of power losses of power transformer of this structure of PV apparatuses [22].

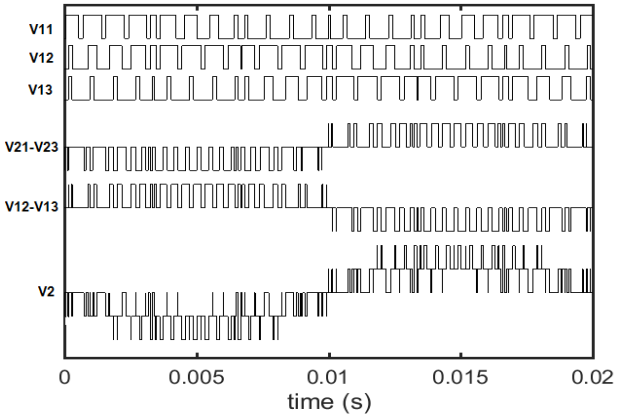

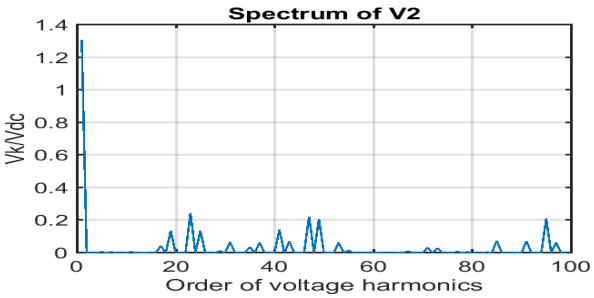

Fig. 23 [22]

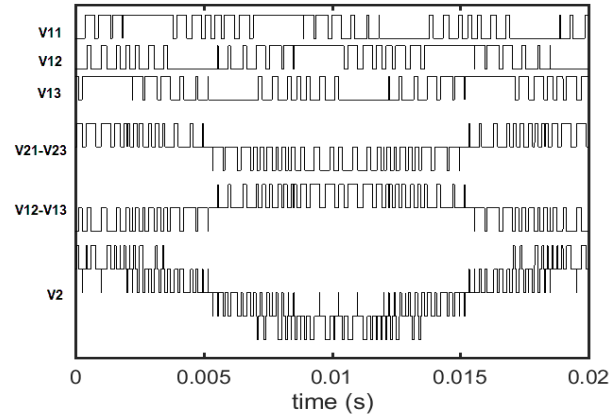

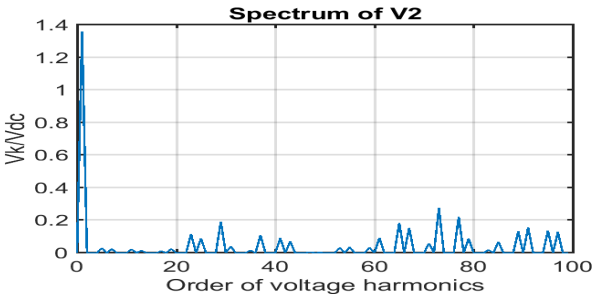

Fig. 24 [22]

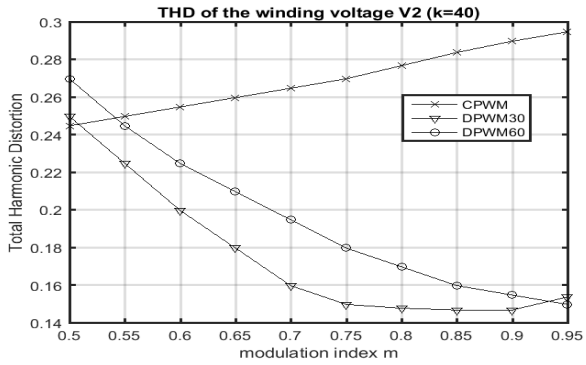

a

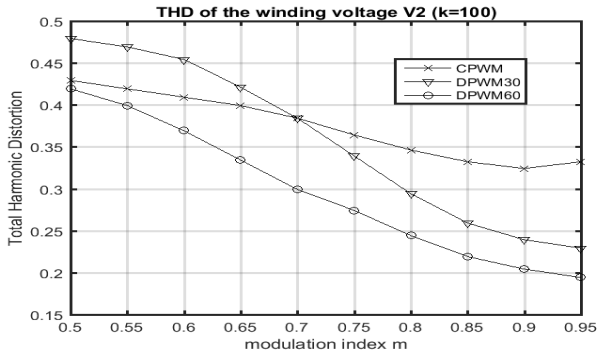

b

Fig. 25 [22]

Conclusion. Development of theory and practice of pulsewidth modulation for power electronic converters began at the end of the 60s – at the beginning of the 70s of the last century. Big efforts of researchers in this field at the end of the 20th century – at the beginning of the 21st century have been concentrated on development of methods and techniques of space-vector-based PWM, which are ones of the most suitable for inverters of drive systems. In order to avoid asynchronous character of standard versions of space-vector PWM, alternative method of synchronous multi-zone modulation, based on space vector approach, has been proposed and developed at the beginning of this century.

The presented review shows some results of development and dissemination of the method of synchronous multi-zone PWM with applications to such perspective topologies of inverter-based systems, as open-end winding motor drives, dual three-phase drive systems, six-phase drives based on four inverters, and two-inverter-based and three-inverter-based photovoltaic installations with increased power level.

It is shown that appropriately modified laws and algorithms of synchronous PWM make it possible to ensure synchronization and symmetry of basic voltage waveforms of the above-mentioned systems over the entire control range, including the overmodulation zone. There are no even harmonics and subharmonics (of the fundamental frequency) in spectra of the base voltages of these power conversion systems. Such an improvement in the harmonic composition of the base voltages and currents in the analyzed inverter-based

systems with synchronous multi-zone modulation, observed under various modes and conditions of their operation, helps to reduce losses in the corresponding installations, and increase their efficiency.

1. Bose B.K. Power electronics, smart grid, and renewable energy systems. Proc. of IEEE. 2017. Vol. 105. No 11. Pp. 2011-2018.

2. Kazmierkowski M.P., Krishnan T., Blaabjerg F. Control in Power Electronics. Academic Press, 2002. 529 p.

3. Holtz J. Pulsewidth modulation for electronic power conversion. Proc. of IEEE. 1994. Vol. 82. No 8. Pp. 1194-1213.

4. Mohan N., Undeland T.M., Robbins W.P. Power Electronics, 3rd edition. John Willey & Sons, 2002. 687 p.

5. Holmes D.G., Lipo T.A. Pulse Width Modulation for Power Converters: Principles and Practice. Wiley-IEEE Press, 2003. 744 p.

6. Tonkal V.E., Lipkovsky K.A., Melnichuk L.P. Ways to improve the quality of the output voltage of autonomous inverters. Kiev: Akademiia nauk UkrSSR, 1972. 92 p. (Rus)

7. Tonkal V.E. Synthesis of autonomous inverters of modulation type. Kiev: Naulova dumka, 1979. 207 p. (Rus).

8. Rudenko V.S., Senko V.I., Chizhenko I.M. Fundamentals of converter technology. Moskva: Vysshaya shkola, 1980. 430 p. (Rus)

9. Kalashnikov B.E., Epshtein I.I. Three-phase autonomous inverters with improved output voltage quality for variable frequency drives. Elektrotehnicheskaya promyshlennost. Preobrazovatelnaya tehnika. 1980. Vypusk 6. Pp. 7 – 9. (Rus).

10. Tonkali V.E., Melnichuk L.P., Novoseltsev A.V., Dyhnenko Yu.I. Semiconductor converters of modulation type with an intermediate link of increased frequency. Kiev: Naukova dumka, 1981. 252 p. (Rus)

11. Grechko E.N., Tonkali V.E. Stand-alone inverters of modulating type. Kiev: Naukova dumka, 1983. 304 p. (Rus)

12. Mykhalskyi V.M. Pulse-width modulation with vector voltage control by autonomous inverters. Pratsi Institutu electrodinamiki Natsionalnoi Akademii nauk Ukrainy. 2010. Vypusk 25. Pp. 105-113. (Ukr)

13. Mykhalskyi V.M. Converting frequencies i voltages with pulse-width modulation: analysis of that scientifically grounded way in increasing the power of electricity. Dissertatsiya…doktora tehn. Nauk. Kyiv, Institute of electrodynamics of NAS of Ukraine, 2010. 488 p. (Ukr)

14. Antonov O.E., Mykhalskyi V.M., Petukhov I.S., Shapoval I.A., Chopik V.V. Ways to improve the efficiency of electromechanical systems and conductor frequency conversion with pulse-width modulation for keruvannya them. Pratsi Institutu electrodinamiki Natsionalnoi Akademii nauk Ukrainy. 2011. Vypusk 29. Pp. 5 – 16. (Ukr)

15. Mykhalskyi V.M. The ability to change the capacity of electricity at the input and output of the frequency and voltage changeover with pulse-width modulation. Kyiv: Institut electrodynamiki NAN Ukrainy. 2013. 340 p. (Ukr)

16. Zagirneak M.V., Klepikov V.B., Kovbasa S.M., Mykhalskyi V.M., Peresada S.M., Sadovoi O.V., Shapoval I.A. Energy efficient electromechanical systems of wide technological application. Kyiv: Institut electrodynamiki NAN Ukrainy, 2018. 310 p. (Ukr)

17. Oleschuk V., Bose B.K., Ovcharenko N., Ermuratski V., Sizov A. Yaroshenko E. Synchronised scheme of high-performance continuous pulsewidth modulation for variable speed drives. *Tekhnichna Elektrodynamika*. 2002. No 4. Pp. 43-48.

18. Oleschuk V., Sizov A., Stankovic A.M., Yaroshenko E. Synchronous control of dual inverter-fed drives with cancellation of zero sequence currents. *Tekhnichna Elektrodynamika*. 2006. No 3. Pp. 13-18.

19. Oleschuk V., Griva G., Prudeak R., Sizov A. Hybrid vehicle drive with synchronously modulated dual inverters. *Tekhnichna Elektrodynamika*. 2009. No 5. Pp. 17-21.

20. Oleschuk V., Sizov A. Synchronous PWM control of four inverters feeding asymmetrical six-phase motor drive. *Tekhnichna Elektrodynamika*. 2011. No 4. Pp. 31-37.

21. Oleschuk V., Griva G., Prudeak R., Sizov A. Dual inverters with synchronized PWM for photovoltaic generation. *Tekhnichna Elektrodynamika*. 2010. No 4. Pp. 8-13.

22. Oleschuk V. Grid-connected PV system employing three inverters regulated by synchronous scheme of PWM. *Tekhnichna Elektrodynamika*. 2022. No 5. Pp. 23-28. DOI: https://doi.org/10.15407/techned2022.05.023

23. Somasekhar V.T., Gopakumar K., Shivakumar E.G., Sinha S.K. A space vector modulation scheme for a dual two level inverter fed open-end winding induction motor drive for the elimination of zero sequence currents. *EPE Journal*. 2002. Vol. 12. No 2. Pp. 22-36.

24. Bojoi R., Tenconi A., Farina F., Profumo F. Dual-source fed multiphase induction motor drive for fuel cell vehicles: topology and control. Proc. of IEEE *Power Electr. Specialists Conf.* Dresden, Germany, 2005. Pp. 2676-2683.

25. Hadiouche D., Baghli L., Rezzoug A. Space-vector PWM techniques for dual three-phase ac machine: Analysis, performance evaluation, and DSP implementation. *IEEE Trans. Ind. Appl*. 2006. Vol. 42. No 4. Pp. 1112–1122.

26. Grandi G., Tani A., Sanjeevkumar P., Ostojic D. Multi-phase multi-level ac motor drive based on four three-phase two-level inverters. Proc. of IEEE Int'l Symp. on *Power Electr., Electr. Drives, Automation and Motion*

(SPEEDAM'2010). Pisa, Italy, 2010. Pp. 1768-1775.
27. Levi E. Advances in converter control and innovative exploitation of additional degrees of freedom for multiphase machines. *IEEE Trans. Ind. Electron*. 2016. Vol. 63. No 1. Pp. 433 – 448.
28. Grandi G., Rossi C., Ostojic D., Casadei D. A new multilevel conversion structure for grid-connected PV applications. *IEEE Trans. Ind. Electron*. 2009. Vol. 56. No 11. Pp. 4416–4426.
29. Oto Y., Noguchi T., Sasaya T., Yamada T., Kazaoka R. Space vector modulation of dual-inverter system focusing on improvement of multilevel voltage waveforms. *IEEE Trans. Ind. Electron*. 2019. Vol. 66. No 12. Pp. 9139-9148.
30. Pires V.F., Cordeiro A., Foito D., Silva J.F. Three-phase multilevel inverter for grid-connected distributed photovoltaic systems based in three three-phase two-level inverters. *Solar Energy*. 2018. Vol. 174. Pp. 1026-1034.

ЕВОЛЮЦІЯ ТА ПОШИРЕННЯ СПЕЦІАЛІЗОВАНИХ СТРАТЕГІЙ, МЕТОДІВ І ТЕХНІК СИНХРОННОЇ ШИРИНО-ІМПУЛЬСНОЇ МОДУЛЯЦІЇ ДЛЯ КЕРУВАННЯ ІНВЕРТОРАМИ ДЖЕРЕЛ НАПРУГИ ТА СИСТЕМАМИ НА ОСНОВІ ІНВЕРТОРІВ

В. Олещук
Institute of Power Engineering of Technical University of Moldova,
Academy Str. 5, Kishinau, MD-2028, Moldova.
E-mail: **oleschukv@hotmail.com**

У роботі подано короткий історичний огляд розвитку методів і техніки широтно-імпульсної модуляції (ШІМ) інверторів джерел напруги, опублікований переважно в українських видавництвах та в українській періодичній пресі. Акцент зроблено на огляді результатів дослідження альтернативних методів і технологій синхронної просторово-векторної багатозонної ШІМ для інверторів з низькою частотою комутації. Зокрема, у зазначених публікаціях основні стратегії, схеми та алгоритми синхронної багатозонної модуляції отримали подальший розвиток, модернізацію, модифікацію та розповсюдження щодо нових перспективних топологій систем перетворення електроенергії, зокрема: двоінверторній – на основі електроприводів з відкритою обмоткою електродвигуна; здвоєні трифазні електроприводи симетричного та несиметричного типу; потужні шестифазні системи на основі чотирьох інверторів, а також фотоелектричні установки на основі двох і трьох інверторів з багатообмотковим трансформатором. Показано, що розроблені схеми та алгоритми синхронної просторово-векторної ШІМ, застосованої для керування інверторними системами, забезпечують безперервну синхронізацію та симетрію основних форм напруги систем у всьому діапазоні керування, включаючи зону перемодуляції інверторів. Це забезпечує мінімізацію парних гармонік і небажаних субгармонік (основної частоти) в спектрах основних напруг систем, що призводить до зменшення втрат в системах і підвищення її ефективності. На основі порівняльного аналізу інтегральних спектральних характеристик фазних і лінійних напруг систем сформульовано рекомендації щодо раціонального вибору схем і алгоритмів синхронної модуляції для відповідних установок залежно від режимів їхньої роботи. Бібл. 30, рис. 25, табл. 2.

Ключові слова: інвертор джерела напруги, стратегія модуляції, привод змінного струму з регульованою швидкістю, фотоелектрична установка, шестифазна система, синхронізація напруги, спектри напруги

Надійшла 24.03.2023
Остаточний варіант 24.04.2023